J. Indian Chem. Soc.,
Vol. 96, November 2019, pp. 1371-1380

The effect of 1:1 boehmite and Y_2O_3 mixed dopant on sintering characteristics, phase assemblage and microstructure of reaction sintered mullite compact derived from bauxite, fly ash and precipitated silica vis a vis individual one

Souvik Dey[a], Arabinda Mondal[b] and Tapan Kumar Parya[c]*

[a]Department of Chemical Technology, Ceramic Engineering Division, University of Calcutta,

92, Acharya Prafulla Chandra Road, Kolkata-700 009, India

[b]Department of Silpa-Sadana, PSV Visva-Bharati University, Santiniketan-731 236, West Bengal, India

[c]Director, School of Engineering and Environmental Sciences, Maulana Abul Kalam Azad University of Technology,

Kolkata-700 064, India

E-mail: mailme.tapan@gmail.com, mailme.tapan2017@rediffmail.com

Manuscript received online 01 July 2019, accepted 16 August 2019

The present investigation has been designed to study on the effect of 1.5% (w/w) 1:1 mixed dopant of boehmite and Y_2O_3 as compared to individual dopant addition on the sintering behavior of stoichiometric mullite compacts at different firing temperatures in between 1400–1575°C. Remarkable thermo-mechanical properties were achieved with co-doped sintered compacts by elimination of pores through rapid particle interaction, orientation and uniform interlocking of the crystallographic phases. Microfine α-alumina particles were observed to be uniformly distributed and adhered to the contact points of well grown interlocked mullite grains via diffusion of ions into the neck areas and filling up of the pores during sintering at 1550°C and above.

Keywords: Mullite, boehmite, Y_2O_3, mixed dopant, microstructure.

Introduction

Stoichiometric mullite and mullite based composite ceramics have attracted keen interest nowadays as multifunctional materials due to its unique thermo-mechanical, chemical, electrical, optical and refractory properties. In the development of novel densified mullite and mullite based composite ceramics, detailed study from the selection of appropriate starting materials, processing route for the precursor, fabrication technique and choice of proper additives to the sintering process and mechanism of solid-state sintering is of utmost scientific necessity. Remarkably low dielectric constant[1] and extraordinary transparency in the mid-infrared region[2] makes mullite into a potential substrate for hi-tech electronic and optical devices.

Depending on starting materials, various processing routes for mullite have been developed such as solid-state sintering, liquid phase sintering, sol-gel, hydrothermal, chemical vapour deposition and spray pyrolysis etc.[3]. Mullites synthesized by liquid phase and solid-state sintering methods are designated as fused-mullite and sinter-mullite respectively[4], while those by other methods are referred to as chemical mullite[4]. In the processing of mullite, different starting materials are used[4]. Mullite properties are greatly influenced by the precursor type and synthesizing method while mechanisms of mullite formation are largely controlled by the method of combining the reactants and mullitization temperatures. The lower mullitization temperature (<1500°C) is needed for precursors derived by sol-gel route vis a vis higher temperature (>1600°C) for mullitization during reaction sintering of powder materials[5].

Naturally occurring minerals contain higher percentage of impurities while sol-gel method generates purified precursor with homogenous morphology attributing higher mulltization rate even at lower sintering temperature[6]. How-

ever, mullite derived from high-purity precursor is quite expensive and not a viable option for its large-scale production due to its low yield and complex processing technique. Therefore, the development of novel mullite body through effective utilization of naturally occurring abundant minerals such as kaolin[7–9], sillimanite[10–12], andalusite[13,14], natural topaz[15], clay[16] poses the key challenge to the scientists.

Johnson[17] investigated the effect of different additives on mullite formation in alumina-silica mixtures to infer that the optimum dopant content to alumina-silica mixtures is essential to maximize mullite formation. Moreover, the degree of effectiveness of different oxides towards mullite formation at a given temperature of firing varies significantly.

Reaction sintering of high aluminous rock, fly ash and reactive silica appears to be an innovative as well as cost-effective method for yielding dense mullite based composite. Earlier communications[18,19] reported the evolution of holistic mullite ceramics from mullite precursors powder based on requisite proportion of bauxite, fly ash and precipitated silica in presence of individual dopant like boehmite and yttria respectively. The pronounced effect of individual sintering aid on sintering temperature, phase assemblage, morphology and thermo-mechanical properties of sintered mullite compacts have been noticed.

Considering the immense scientific and technological importance of mullite and its composites and keeping in view all the parameters cited above, the present investigation has been designed to evolve dense stoichiometric mullite and mullite based composite from the precursors consisting of bauxite, fly ash and precipitated silica in presence of mixed dopants during sintering between 1400–1575°C. The mixed dopant content to the batch has been kept restricted purposefully at 1.5% (w/w) only for minimizing the changes in the grain boundary chemistry of formed mullite and its composites. Finally, a comprehensive attempt has been undertaken to compare mixed effect of boehmite and Y_2O_3 against that of individual sintering aid on the sintering temperature, phase assemblage, microstructure evolution and thermo-mechanical properties of such mullite compacts.

Experimental

Refractory grade bauxite (Saurashtra, Gujarat), fly ash (Bakreswar Thermal Power Plant, West Bengal) and precipitated silica (synthesized) were selected as starting materials. In order to maintain the exact molar ratio of Al_2O_3/SiO_2 as 3:2 in mullite precursor, the requisite proportion of bauxite, fly ash and precipitated silica were taken. Table 1 summarized the chemical composition of bauxite, fly ash and precipitated silica in wt% respectively. On the basis of the chemical analyses of the starting materials, batch composition and oxide equivalent of stoichiometric mullite were computed. The chemical analysis of bauxite exhibited a high alumina content with low percentages of associated impurities. Fly ash analysis revealed the presence of high silica and moderate alumina content with the controlled amount of iron oxide, lime and magnesia respectively. The chemical analyses of above starting materials confirmed the impurities content were within a reasonable limit and would not grossly affect the prospective properties of fired mullite compact.

At first, bauxite was crushed, ground and subsequently sieved through BS 100 mesh. The requisite proportion of the powder raw materials as per the batch (Table 2) were wet milled in a rapid pot mill using alumina balls for 10 h. The slurry was then thoroughly dried at 110°C for 24 h, calcined at 600°C for 2 h followed by grinding of the agglomerate to a fine powder. The powder was finally sieved through BS 150 mesh. Different batches were prepared by intimate mixing of above stoichiometric precursor of mullite through the incorporation of boehmite and Y_2O_3 in the proportion of 1.5% (w/w) respectively in a high-speed planetary mixer. Another batch precursor of mullite containing 1.5% (w/w) of an equal proportion of both boehmite and yttria was also prepared.

Table 1. Chemical analysis of the raw materials (wt%)

Raw materials	Constituents							
	Al_2O_3	SiO_2	Fe_2O_3	MgO	CaO	TiO_2	Alkali (Na_2O+K_2O)	LOI
Bauxite	60.30	2.90	1.85	–	1.69	0.51	0.20	32.55
Fly ash	29.61	63.45	2.50	2.05	1.41	–	–	0.99
Precipitated silica	–	86.55	–	–	–	–	Trace	13.40

Table 2. Batch compositions of mullite precursor (wt%) in presence of sintering aids

Raw materials	Batch composition		
	A	B	C
Refractory grade bauxite	74.37	74.37	75.57
Fly ash	17.23	17.23	16.53
Precipitated silica	6.90	6.90	6.40
Synthetic boehmite	1.50	–	0.75
AR grade Y_2O_3	–	1.50	0.75

From the batch powder, rectangular bars (72 mm×11 mm ×8 mm) were fabricated by uni-axial pressing in a hydraulic press at the pressure of 150 MPa and dried at 110°C for 24 h in an air oven. Finally, the dried bars were fired at 1400–1575°C in a programmable muffle furnace with fixed 4 h soaking time in each case.

Densification behavior of the respective sintered samples was evaluated by measuring firing shrinkage, bulk density, apparent porosity, modulus of rupture, thermal shock resistance and residual strength after spalling. The sintered products were also tested for phase assemblage by XRD and microstructure by SEM study. Linear firing shrinkage was studied by measuring the dimensional change of the bars before and after firing (ASTM C179-14). Bulk density and apparent porosity were determined by conventional liquid displacement method using Archimedes' principle in water medium (ASTM C20-00(2015)). The flexural strength of fired compacts was measured by three-point bending method (ASTM C1161-13) in instrument LRX, version 2.13, Lloyd, UK. Thermal shock resistance was measured by putting the fired bar compacts at 1000°C in an electric muffle furnace for 10 min followed by in the air for 10 min to complete one cycle. After 20 cycles of spalling, the residual strength was measured by three-point bending method (ASTM C1161-13). The powder XRD pattern of the fired sample was recorded over Bragg's angle 2θ from 10–60° in a Philips X-ray diffractometer (X'Pert PRO PW-3071) using Ni-filter Cu-Kα radiation at the scanning rate of 2°/min. Microstructural characterization on an etched surface of samples sintered at different temperatures was performed in Scanning Electron Microscope (ZEISS, INCA Penta FETx3, MODEL, EDS8100, UK) at magnification of 15.00 KX.

Results and discussion

The chemical analyses of the starting materials, as well as batch compositions used in the study, have been given in Table 1 and Table 2 respectively. The oxide compositions of different mullite batch precursors are also presented in Table 3.

A constant molar ratio for Al_2O_3 and SiO_2 as 3:2 is maintained although minor percentages of Fe_2O_3, CaO, TiO_2 and alkalies (Na_2O + K_2O) are present as impurities. Al_2O_3 content of around 51% (w/w) and SiO_2 content around 18.2% (w/w) were noted in the batch precursor.

All the samples fired at temperatures between 1400°C to 1575°C are grayish-white in appearance and exhibit smooth texture without any visible distortion or crack.

Linear firing shrinkage:

The changes of firing shrinkage (%) against firing temperature and dopant content is graphically represented in Fig. 1. It is evident from Fig. 1 that with increasing firing temperature of firing from 1400°C to 1575°C, the linear shrinkage of the compacts increased continuously[18]. The increase in linear shrinkage with the rise in firing temperature is owing to densified mullitization of amorphous silica with transition alumina with the removal of pores and coalescence of the grains[19].

Initially, the glassy phase is progressively consumed by alumina to yield more mullite at the higher temperature of firing. In addition, mullite grains tend to grow in size. The mixed dopant added fired samples exhibit a slightly higher degree of firing shrinkage than that of boehmite containing mullite body in the firing range of 1500°C to 1575°C. Maxi-

Table 3. Oxide composition of different mullite batch precursors (wt%)

Batch No.	Oxide composition								
	Al_2O_3	SiO_2	Fe_2O_3	MgO	CaO	TiO_2	Y_2O_3	Alkali (Na_2O+K_2O)	LOI
A	51.97	18.22	1.81	0.34	1.51	0.39	–	0.15	25.63
B	50.47	18.22	1.81	0.34	1.51	0.39	1.50	0.15	25.60
C	51.23	18.22	1.81	0.34	1.51	0.39	0.75	0.15	25.62

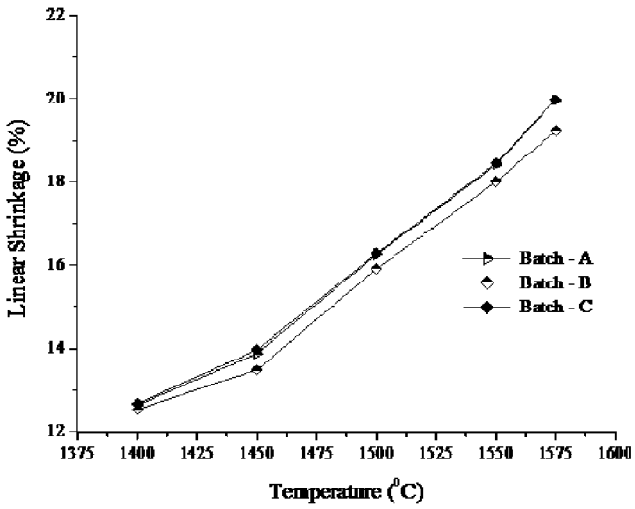

Fig. 1. Variation of linear shrinkage (%) with temperature (°C) of sintered compacts.

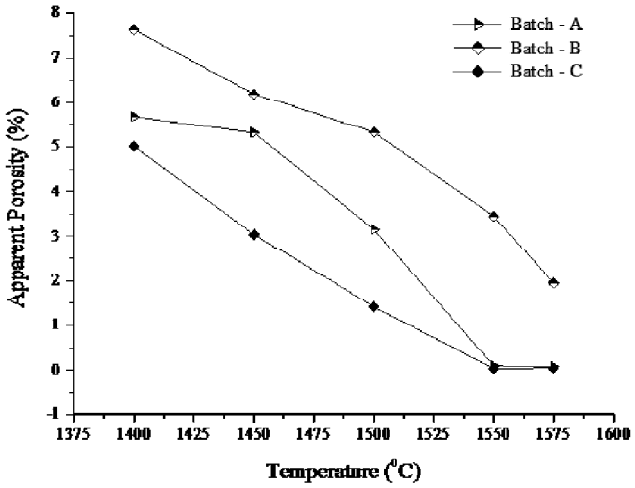

Fig. 3. Variation of apparent porosity (%) with temperature (°C) of sintered compacts.

mum firing shrinkage value of 19.99% is obtained in the co-doped mullite compact during firing at 1575°C indicating rapid material interaction, transportation and interlocking of the grains with consequent removal of open pores.

Bulk density and apparent porosity:

The variation in bulk density vis-a-vis apparent porosity of sintered mullite bodies against firing temperature is shown in Fig. 2 and Fig. 3 respectively.

It is evident from the Fig. 2, that the bulk density of sintered compacts increases sharply with a simultaneous significant reduction of apparent porosity during firing from 1400°C to 1575°C. Active alumina in synthetic boehmite[18] tends to react with cristobalite readily to generate mullite even at a lower temperature of 1550°C which is responsible of high bulk density with corresponding elimination of open porosity in sintered compact as compared to yttria addition. With the addition of Y_2O_3, mullite grains tend to grow large enough to come closer with adjacent grains leaving behind few voids at the multigrain junctions[19]. The pores are simultaneously filled up with yttrious silicate glass. Since, the extent of formation of yttrious silicate glass is directly proportional to the Y_2O_3 addition, a significant reduction in porosity has been observed with increasing addition of Y_2O_3. With the increase in firing temperature and Y_2O_3 content in the composition, more and more densification is found to occur since, at this stage, material transport by both lattice and grain boundary diffusion predominates[19].

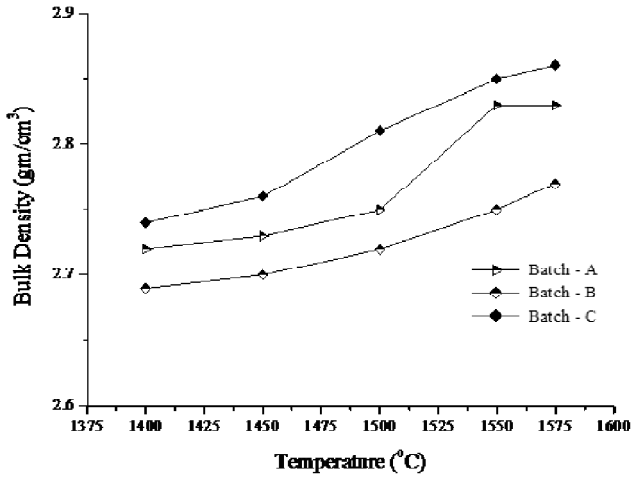

Fig. 2. Variation of bulk density (g/cm^3) with temperature (°C) of sintered compacts.

With co-doping of boehmite and yttria, corundum particles are readily formed and adhered to the contact points of mullites thereby favoring diffusion of ions in the neck areas and filling up of the pores. This causes a substantial reduction in porosity value to 0.05% only of the sintered compact with simultaneously high bulk density value of 2.86 g/cc.

Modulus of rupture:

Fig. 4 shows the variation of bending strength against sintering temperature. As compared to yttria addition, boehmite addition results in high bending strength which may be due to the uniform distribution and interlocking of secondary

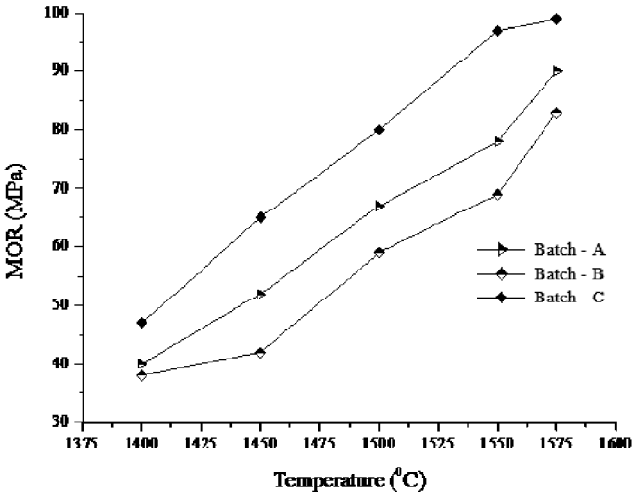

Fig. 4. Variation of bending strength (MPa) with temperature (°C) of sintered compacts.

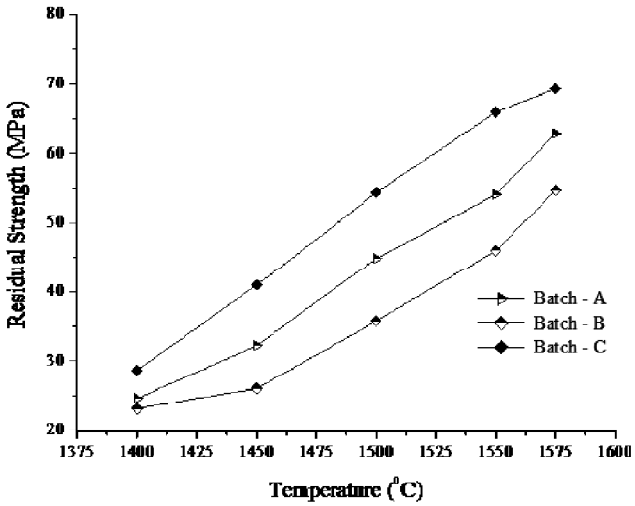

Fig. 5. Variation of residual strength (MPa) with temperature (°C) of sintered compacts.

mullite grains throughout the matrix during sintering at 1575°C[18]. Yitria greatly promotes densification by sealing the voids and forming interlocked mullite grains within the matrix[19].

The significant influence of co-doping towards the remarkable improvement of flexural strength as high as 99 MPa was observed.

Thermal shock resistance and residual strength:

The sintered samples are subjected to repeated heating and cooling cycles at 1000°C. After 20 cycles of spalling, no micro-crack or distortion in all samples is noted. Fig. 5 illustrates the variation of residual flexural strength after 20 cycles of spalling operation for each set, which focuses on the substantial retention of significant flexural strength over 60% of initial strength in respective body probably due to stronger ceramic-ceramic bonds amongst interlocked mullite grains.

The retention of considerably high flexural strength (69.30 MPa) of sintered samples containing mixed additive even after 20 cycles of thermal spalling operation confirms the outstanding thermal stability of the co-doped sintered body.

Crystalline phase analysis by XRD:

For Batch A sample on firing at 1400°C exhibits mullite (PDF No. 15-0776) as major crystalline phase along with cristobalite (PDF No. 82-1409) as minor phase. Fig. 6 clearly reveals that cristobalite phase disappears gradually while crystallinity of mullite phase increases progressively with the rise in firing temperature up to 1575°C as evident from the sharp rise of the relative intensity of characteristic peaks.

This fact may be explained by initial dissolution of *in situ* formed alumina within the transitory liquid phase leading to saturation and subsequent precipitation of secondary mullite crystals. In presence of synthetic boehmite and on firing above 1400°C, rapid mullitization occurs by intense interaction of the reactive alumina and cristobalite leading to the formation of primary mullite as major phase and secondary mullite as a minor phase in contact with liquid phase derived from the impurities of fly ash and bauxite. It is presumed that in presence of reactive alumina, random nucleation of mullite seeds occurs. With an increase of temperature of heat treatment from 1400–1575°C, mullite phase becomes more and more pronounced with lesser or negligible proportion of cristobalite content. At the same time, the prominent existence of corundum phase is visible particularly in the batches fired at 1550°C and above.

In presence of yttria, with the progressive rise in firing temperature, cristobalite phase also starts forming and eventually mullite phase predominates over cristobalite giving rise to sharp mullite peaks (Fig. 7). No sharp characteristic peak of $Y_2Si_2O_7$ phase is noticed which might be dissolved in the glassy matrix with a resultant decrease in viscosity.

Investigation reveals that extensive mullitization occurs from liquid phase sintering of yttrious silicate glass. The dissolution of alumina particles makes the glass saturated with alumina followed by separation of secondary mullite crystal.

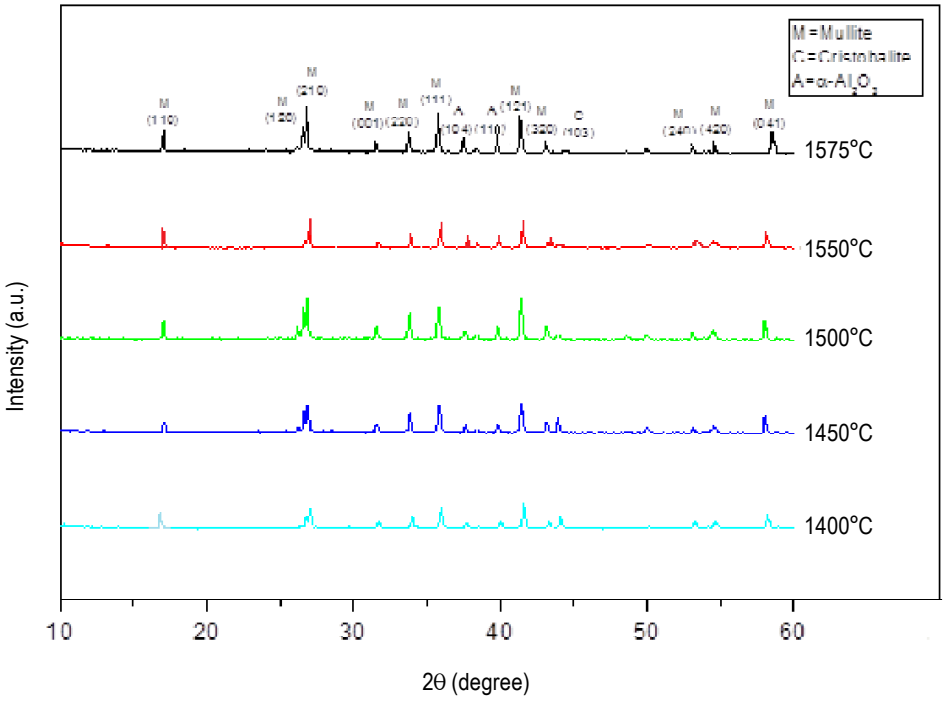

Fig. 6. Powder XRD patterns of Batch A sintered compacts fired at different temperatures (M is Mullite, C is Cristobalite and A is α-Al_2O_3).

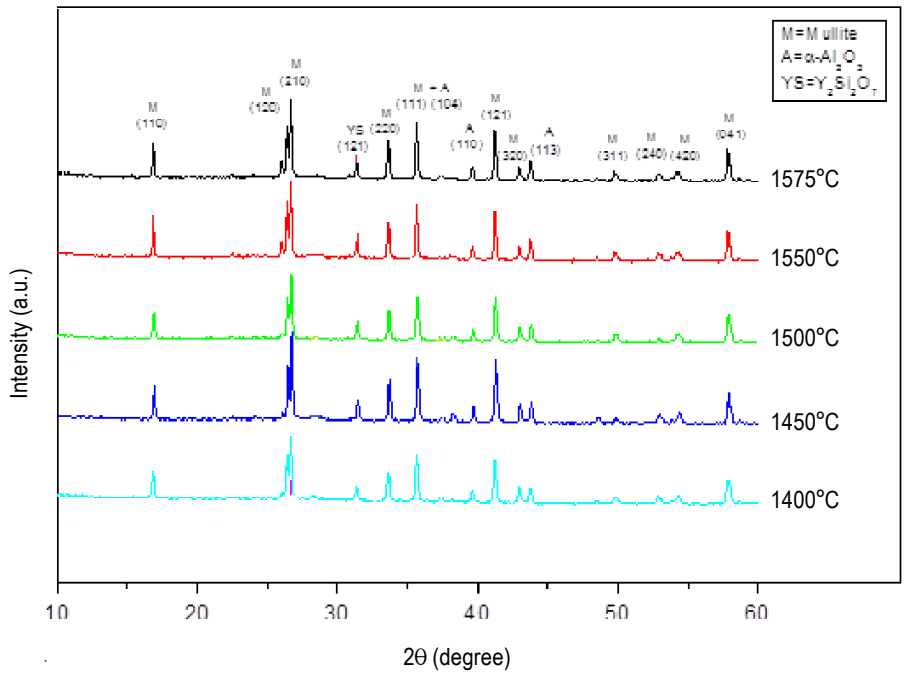

Fig. 7. Powder XRD patterns of Batch B sintered compacts fired at different temperatures (M is Mullite, C is Cristobalite, A is α-Al_2O_3 and YS is $Y_2Si_2O_7$).

The growth of mullite is intrinsically related to the dissolution of alumina into the glass. With the growth of mullite crystal, depletion of siliceous phase occurs with corresponding increase in the yttrious silicate glass phase and ultimately leads

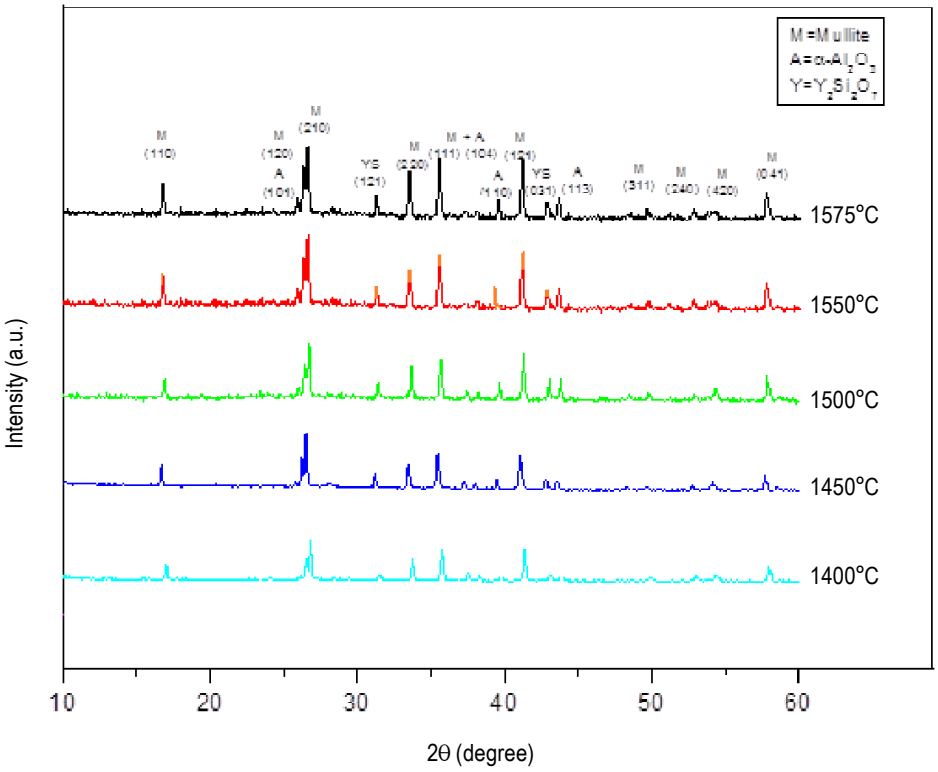

Fig. 8. Powder XRD patterns of Batch C sintered compacts fired at different temperatures (M is Mullite, C is Cristobalite, A is α-Al_2O_3 and YS is $Y_2Si_2O_7$).

to the formation of the crystalline $Y_2Si_2O_7$ phase (PDF No. 38-0223) which is confirmed by the XRD patterns where complete depletion of cristobalite phase has been recorded during firing at 1550°C and above.

With co-doping of 1.5% 1:1 synthetic boehmite and yttria during firing at 1575°C, the peaks of well-crystalline mullite and intensive peaks of corundum as major phases has been noticed (Fig. 8).

Microstructure by SEM:

The SEM micrographs of the etched surface of each sample sintered at different temperatures were presented in Figs. 9–11. With incorporation of boehmite, enhanced formation of granular MII type[20] secondary mullite (Fig. 9[a]) with lower aspect ratio along with few MIII type[20] secondary mullite are found (Fig. 9[b]).

Microfine active Al_2O_3 from boehmite augments the solid-state inter-diffusion rate[21] and thereby facilitating the growth of the mullite seeds. The boehmite addition to the mullite batches favors uniform size distribution of mullite grains which result in maximization of density and reduction of porosity[22] without much grain growth. Fig. 9[c] showed existence of corundum grains of size ~ 40 nm adhered to contact points of mullites favoring diffusion of ions with growth in the neck areas thereby filling up the pores.

The grain sizes of mullite in Y_2O_3 containing compacts are comparatively larger than that of boehmite doped sintered compacts at any given temperature of firing (Fig. 10). The disordered layer of yttrious silicate may trigger up the mobility of the boundaries resulting in controlled grain growth which instead of developing anisotropy or faceted structure has accomplished random morphologies of secondary mullite with curved grain boundaries (Fig. 10[a] and Fig. 10 [b]). The yttrious silicate, in turn, leads to precipitation of excess microfine alumina in the batch and is entrapped within the well-grown mullite grains (Fig. 10[c]) through lowering the Al_2O_3/SiO_2 molar ratio at the sintering temperature of 1550°C and 1575°C.

Microfine α-alumina particles are being embedded into the interlocked mullite grains in the SEM micrograph (Fig. 11) of the sintered body at 1575°C.

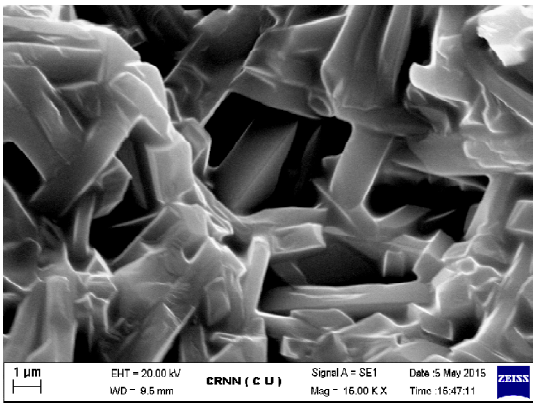

(a)

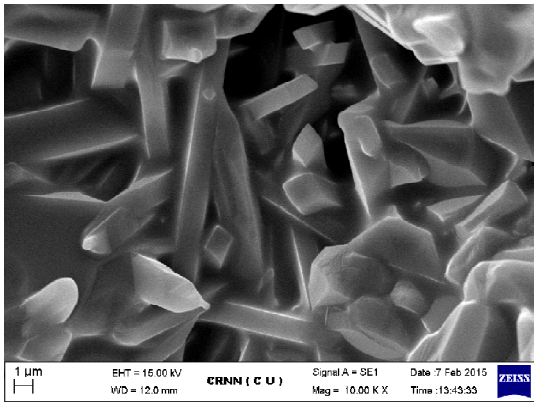

(b)

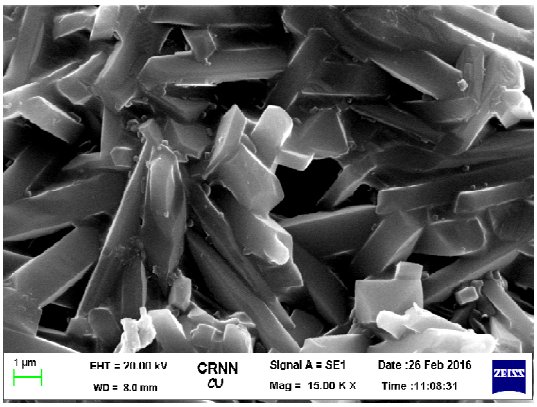

(c)

Fig. 9. SEM micrographs of Batch A sintered compacts fired at different temperatures: (a) 1450°C, (b) 1550°C and (c) 1575°C respectively.

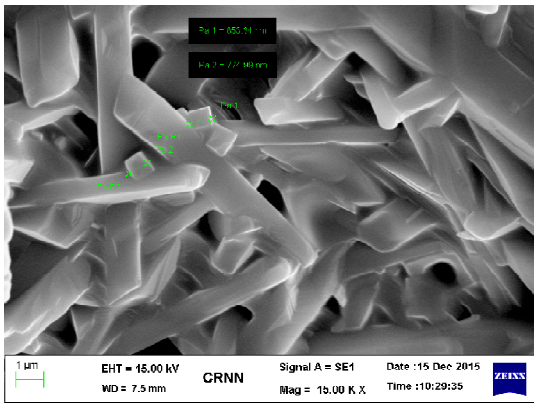

(a)

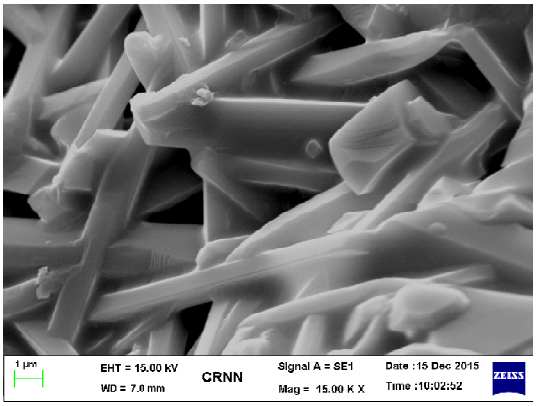

(b)

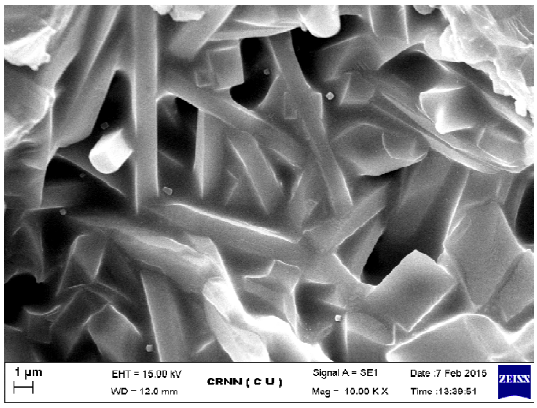

(c)

Fig. 10. SEM micrographs of Batch B sintered compacts fired at different temperatures: (a) 1450°C, (b) 1550°C and (c) 1575°C respectively.

In presence of 1.5% (w/w) 1:1 boehmite and yttria, Rietveld analysis of the fired compacts at 1575°C exhibited 96.20% mullite and 2.30% corundum without any cristobalite phases. EDAX of the fired samples clearly supported the

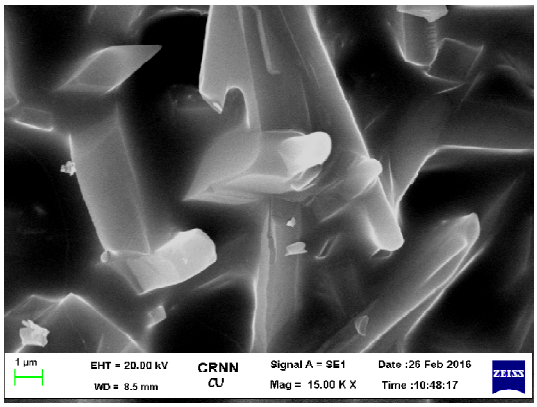

(a)

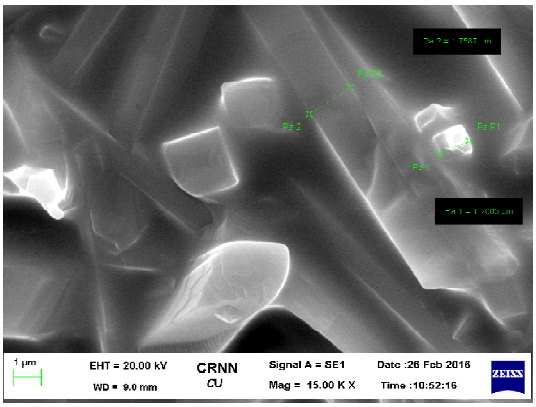

(b)

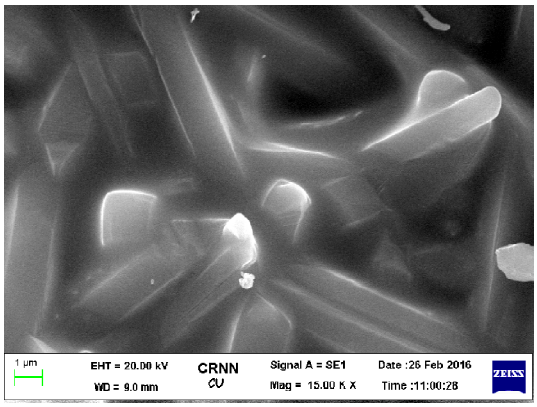

(c)

Fig. 11. SEM micrographs of Batch C sintered compacts fired at different temperatures: (a) 1450°C, (b) 1550°C and (c) 1575°C respectively.

formation of secondary mullite with separation of α-alumina phase from Al_2O_3-rich primary mullite.

Conclusion

From this investigation, the following conclusions can be drawn:

(i) Cost effective mullite ceramics can be evolved by conventional reaction sintering of indigenous starting materials based on natural bauxite, fly ash and precipitated silica at a relatively lower temperature. The combined doping action of boehmite and Y_2O_3 on the densification behavior and morphological evolution of mullite are well evidenced.

(ii) The significant improvement in thermo-mechanical properties and dense microstructure in reaction sintered mullite bodies containing 1.5% (w/w) of 1:1 boehmite and yttria boehmite have been accomplished during sintering at 1550°C and above.

(iii) Addition of Y_2O_3 favors the formation of yttrious silicate glassy phase at the grain boundary which initially accelerates dissolution of alumina particles followed by nucleation and controlled growth of mullite grains thereby resulting in drastic reduction of apparent porosity in the fired mullite compacts.

(iv) Significant improvement in bulk density, flexural strength, strength retention after thermal spalling vis-a-vis dense interlocked microstructure of *in situ* formed mullite grains with the addition of 1.5% (w/w) yttria has been occurred during sintering at 1550–1575°C. Therefore, Y_2O_3 acts as a normal grain growth accelerator in sintering of mullite and mullite based composites.

(v) The outstanding thermo-mechanical properties and homogeneous microstructure of mullite have been accomplished during sintering of co-doped compacts at 1575°C where only 0.75% boehmite and 0.75% Y_2O_3 are incorporated as a mixed dopant.

(vi) Pronounced doping action of 1.5% (w/w) 1:1 boehmite and Y_2O_3 towards the effective consolidation and the homogeneous microstructural features of mullite based composites fired at 1550°C and above has exclusively been proved than that of individual one.

References

1. I. A. Aksay, D. M. Dabbs and M. Sarikaya, *J. Am. Ceram. Soc.* 1991, **74(10)**, 2343.

2. H. Schneider, M. Schmücker, K. Lkeda and W. A. Kaysser, *J. Am. Ceram. Soc*., 1993, **76(11)**, 2912.
3. O. Aladesuyi, M. Pal, S. K. Das and K. O. Ajanaku, *J. Mater. Environ. Sci.*, 2017, **8(8)**, 2832.
4. H. Schneider, J. Schreuer and B. Hildmann, *J. Eur. Ceram. Soc*., 2008, **28(2)**, 329.
5. S. M. Johnson and J. A. Pask, *Am. Ceram. Soc. Bull*., 1982, **61(8)**, 838.
6. J. Sanz, I. Sobrados, A. L. Cavalieri, P. Pena, S. de Aza and J. S. Moya, *J. Am. Ceram. Soc*., 1991, **74(10)**, 2398.
7. C. Y. Chen, G. S. Lan and W. H. Tuan, *J. Eur. Ceram. Soc*., 2000, **20(14-15)**, 2519.
8. M. A. Sainz, F. J. Serrano, J. M. Amigo, J. Bastida and A. Caballero, *J. Eur. Ceram. Soc*., 2000, **20(4)**, 403.
9. J. Temuujin, K. J. D. MacKenzie, M. Schmücker, H. Schneider, J. McManus and S. Wimperis, *J. Eur. Ceram. Soc*., 2000, **20(4)**, 413.
10. H. S. Tripathi and G. Banerjee, *Ceram. Int*., 1999, **25(1)**, 19.
11. S. Rahman, U. Feustel and S. Freimann, *J. Eur. Ceram. Soc*., 2001, **21(14)**, 2471.
12. C. H. Rüscher, *J. Eur. Ceram. Soc*., 2001, **21(14)**, 2463.
13. M. L. Bouchetou, J. P. Ildefonse, J. Poirier and P. Daniellou, *Ceram. Int*., 2005, **31(7)**, 999.
14. M. Sardy, A. Arib, K. El Abbassi, R. Moussa and M. Gomina, *New J. Glass Ceram*., 2012, **2(3)**, 121.
15. X. Miao, *Mater. Lett*., 1999, **38(3)**, 167.
16. V. Viswabaskaran, F. D. Gnanam and M. Balasubramanian, *Ceram. Int*., 2002, **28(5)**, 557.
17. S. M. Johnson, "Mullitization of Kaolinite and Al_2O_3-SiO_2 mixtures", Technical Information Department, Lawrence Berkeley National Laboratory, University of California, 2012, pp. 1-61.
18. S. Dey, D. Ray, A. Mondal and T. K. Parya, *Refractories World Forum*, 2016, **8(4)**, 85.
19. S. Dey, D. Ray, A. Mondal and T. K. Parya, *Ceram. Int*., 2018, **44(9)**, 10087.
20. Y. Iqbal and W. E. Lee, *J. Am. Ceram. Soc*., 2000, **83(12)**, 3121.
21. Y. Chen, M. Wang and M. Hon, *J. Mater. Research*, 2004, **19(3)**, 806.
22. V. Viswabaskaran, F. D. Gnanam and M. Balasubramanian, *Appl. Clay Sci.*, 2004, **25(1-2)**, 29.